



# Stereolithographic Rapid Prototyping of Clear, Foldable, Non-Refractive Intraocular Lens Designs: A Proof-of-Concept Study

Veronica Hidalgo-Alvarez, Noelia D. Falcon, Julie Eldred, Michael Wormstone & Aram Saeed

To cite this article: Veronica Hidalgo-Alvarez, Noelia D. Falcon, Julie Eldred, Michael Wormstone & Aram Saeed (19 May 2024): Stereolithographic Rapid Prototyping of Clear, Foldable, Non-Refractive Intraocular Lens Designs: A Proof-of-Concept Study, Current Eye Research, DOI: [10.1080/02713683.2024.2344164](https://doi.org/10.1080/02713683.2024.2344164)

To link to this article: <https://doi.org/10.1080/02713683.2024.2344164>



© 2024 University of East Anglia. Published with license by Taylor & Francis Group, LLC



[View supplementary material](#)



Published online: 19 May 2024.



[Submit your article to this journal](#)



Article views: 1236



[View related articles](#)



[View Crossmark data](#)

# Stereolithographic Rapid Prototyping of Clear, Foldable, Non-Refractive Intraocular Lens Designs: A Proof-of-Concept Study

Veronica Hidalgo-Alvarez<sup>a#</sup>, Noelia D. Falcon<sup>a#</sup>, Julie Eldred<sup>b</sup>, Michael Wormstone<sup>b</sup> and Aram Saeed<sup>a</sup> 

<sup>a</sup>School of Pharmacy, University of East Anglia, Norwich, UK; <sup>b</sup>School of Biological Sciences, University of East Anglia, Norwich, UK

## ABSTRACT

**Purpose:** A cataract is a cloudy area in the crystalline lens. Cataracts are the leading cause of blindness and the second cause of severe vision impairment worldwide. During cataract surgery, the clouded lens is extracted and replaced with an artificial intraocular lens, which restores the optical power. The fabrication of intraocular lenses using existing molding and lathing techniques is a complex and time-consuming process that limits the development of novel materials and designs. To overcome these limitations, we have developed a stereolithography-based process for producing models of clear lens designs without refractive function, serving as a proof of concept. This process has the potential to contribute toward new lens development, allowing for unlimited design iterations and an expanded range of materials for scientists to explore.

**Methods:** Lens-like 3D objects without refractive function were fabricated by using stereolithography. A photopolymerizable resin containing 2-phenoxyethyl acrylate, poly (ethylene glycol) dimethacrylate, and a suitable photoinitiator was developed for the production of lens-like 3D object prototypes. The morphology of the printed devices was characterized by scanning electron microscopy. The transparency and thermal properties were analyzed using spectrophotometry and differential scanning calorimetry, respectively. The biocompatibility of the devices was investigated in a cultured human lens cell line (FHL-124), using a standard lactate dehydrogenase assay, and the lenses were folded and implanted in the human capsular bag model.

**Results:** One-piece lens-like 3D objects without refractive function and with loop-haptic design were successfully fabricated using Stereolithography (SLA) technique. The resulting 3D objects were transparent, as determined by UV spectroscopy. The lactate dehydrogenase test demonstrated the tolerance of lens cells to the prototyping material, and apparent foldability and shape recovery was observed during direct injection into a human capsular bag model *in vitro*.

**Conclusions:** This proof-of-principle study demonstrated the potential and significance of the rapid prototyping process for research and development of lens-like 3D object prototypes, such as intraocular lenses.

## ARTICLE HISTORY

Received 11 January 2024  
Accepted 11 April 2024

## KEYWORDS



Cataract; refractive surgery; 3D printing of intraocular lenses; intraocular lens; optics

## Introduction

Cataract, a cloudiness of the crystalline lens, is the leading cause of blindness worldwide.<sup>1,2</sup> More than 50% of all blindness is caused by this pathology, with a higher prevalence among elderly populations. Consequently, the incidence of cataract is only expected to rise due to the increasing life expectancy in developed countries.<sup>1</sup> Currently, the only effective treatment for cataract is surgery.<sup>3</sup> During a cataract operation, a circular opening (~5 mm diameter) is made in the anterior capsule of the lens by performing the capsulorhexis technique. The cataractous lens fibers are then emulsified and extracted *via* phacoemulsification.<sup>4</sup> A capsular bag is thus generated, comprising part of the anterior capsule and the entire acellular posterior capsule.<sup>2</sup> An artificial intraocular lens (IOL) is then implanted within this structure to

restore the refractive power of the natural lens.<sup>5</sup> Following this procedure, light can pass freely through the transparent implanted IOL and the thin, acellular posterior capsule.<sup>6</sup> This allows the formation of a high-quality visual image in the retina and the subsequent improvement in visual acuity.<sup>7,8</sup>

IOLs are formed of an optic component that sits within the visual axis and provides the refractive properties, and haptics that provide support and stability within the capsular bag.<sup>9</sup> Currently, a wide variety of materials are used in the fabrication of IOLs. These can be rigid hydrophobic polymers, such as polymethylmethacrylate (PMMA), or flexible materials, such as acrylics, silicones, and hydrogels.<sup>10</sup> The use of flexible biomaterials with a high refractive index allows the implantation of the IOL through a smaller incision, which is less disruptive to the eye and is associated with lower post-surgical inflammation. Therefore, it is

**CONTACT** Aram Saeed  [aram.saeed@uea.ac.uk](mailto:aram.saeed@uea.ac.uk)  School of Pharmacy, University of East Anglia, Norwich Research Park, Norwich, NR4 7TJ, UK

<sup>#</sup>These authors contributed equally to this work and are co-first authors.

Research Center for Life Science and Healthcare, Nottingham Ningbo China Beacons of Excellence Research and Innovation Institute (CBI), University of Nottingham Ningbo China, Ningbo 315000, China

 Supplemental data for this article is available online at <https://doi.org/10.1080/02713683.2024.2344164>

© 2024 University of East Anglia. Published with license by Taylor & Francis Group, LLC

This is an Open Access article distributed under the terms of the Creative Commons Attribution License (<http://creativecommons.org/licenses/by/4.0/>), which permits unrestricted use, distribution, and reproduction in any medium, provided the original work is properly cited. The terms on which this article has been published allow the posting of the Accepted Manuscript in a repository by the author(s) or with their consent.

preferable to implant a foldable IOL rather than a rigid one.<sup>9</sup> Similarly, there are different IOL designs that are made for implantation in different parts of the anterior segment of the eye. These include single- or multi-piece configurations, plate-haptic or open-loop styles, and angulated or planar haptic designs.<sup>11,12</sup>

The main methods used in the manufacture of IOLs include molding and lathing.<sup>13,14</sup> Molded IOLs are produced by pouring a polymerizable resin into a mold and heating it to induce the thermal polymerization of the material.<sup>13</sup> On the other hand, lathing involves the production of rods that are cut into disc-shaped structures which are then machined with a lathe to produce the IOL.<sup>15,16</sup> Once formed, the IOLs are polished to remove any artifacts that may compromise the smoothness of the IOL surfaces while preserving the sharp edges.<sup>13,14</sup> While the utilization of these manufacturing techniques results in the production of high-quality IOLs, they also have numerous disadvantages, especially when prototyping new IOL designs. First, these methods are particularly time-consuming, as they require highly demanding cleaning procedures and the execution of multiple steps.<sup>17</sup> In the case of molding, artifacts can form around the edge of the IOLs due to polymer spillage from the molds. These could cause damage to intraocular tissues if not removed before implantation.<sup>18</sup> Another issue is the high cost associated with the use of specialist equipment that often needs replacement due to damage and wear.<sup>17</sup> These limitations make it desirable to seek faster and more cost-effective techniques for the production of IOLs.

Additive manufacturing allows the fabrication of objects designed on computer-aided design (CAD) software by depositing materials layer by layer until the whole structure is formed.<sup>19,20</sup> Of the different types of additive manufacturing technology currently available, SLA is usually the method of choice for the fabrication of lenses.<sup>21</sup> There are many advantages to this process, including a high resolution and speed of fabrication, the versatility of the materials that can be used, and the possibility of using them simultaneously.<sup>22</sup> These attributes make SLA a promising technique to accelerate the production of novel IOL prototypes.

While previous studies have attempted to use additive manufacturing to produce IOLs, none have reported the fabrication of a structure that is representative of a commercial model and the analysis of the physico-chemical, mechanical, and biological properties of a specific prototype.<sup>23–25</sup> We report herein a method for the production and characterization of lens-like 3D objects *via* SLA using a photopolymerizable formulation developed in house. The use of this material allowed the production of transparent devices which had the mechanical properties required for this type of implant. The cytocompatibility of the material was tested *in vitro*, proving that the polymer did not elicit toxic responses upon lens epithelial cells. Thus, this proof-of-concept study showed that lens-like 3D objects could potentially be produced with materials that are used for SLA, although care should be taken to choose the appropriate technology. Furthermore, a set of characterization techniques was established and adapted for the analysis of the printed implants

using non-specialist equipment. The findings suggest that the process requires refinement and additional testing before considering its application for the manufacture of refractive intraocular lenses (IOLs). However, it remains suitable for producing prototypes, potentially aiding researchers in the development of innovative therapeutic implants to address specific clinical challenges.

## Materials and methods

### Design and fabrication of IOL-like implants using SLA

The CAD model of the lens-like 3D objects without refractive function was created using Blender (Stichting Blender Foundation, Amsterdam, The Netherlands) as a modeling software. The model was based on a one-piece design with an optic component and looped haptics. The haptic-to-haptic length was 13 mm, the optic diameter was 6 mm, and the thickness was set at 0.9 mm. The model was exported and saved in STL format for SLA printing, which allowed direct import into SLA software of a commercially available SLA printer.

The photopolymerizable mixture was prepared by mixing 93% (w/w) 2-phenoxyethyl acrylate (>93% purity, TCI Chemicals, Tokyo, Japan), 7% (w/w) poly (ethylene glycol) dimethacrylate ( $M_n$  750 Da, Sigma-Aldrich, UK), and an additional amount equivalent to 1% (w/w) of diphenyl (2,4,6-trimethylbenzoyl) phosphine oxide (>98% purity, TCI Chemicals, Tokyo, Japan) in proportion to the total mass of the starting materials was added to the mixture. The mixture was stirred in the dark and purged with nitrogen for ~20 min. A suitable amount of the liquid resin was then poured onto the resin tank of the SLA printer and polymerized in a single layer *via* repeated exposure to the UV light (405 nm, 250 mW) integrated into the printer. The exposure time of the resins to the UV light was optimized to ensure that the IOL structure was formed while avoiding over-curing effects. The resulting devices were washed with isopropanol and post-cured by irradiating them with UV light for 1 h and heating in a vacuum oven at 70 °C overnight. The efficiency of the post-curing process was investigated by <sup>1</sup>H NMR, as this allowed the detection of any monomers that leached from implants that had or had not been post-cured and the subsequent comparison between the different experimental groups (Supplementary Information). The dimensional accuracy of the printed implants was calculated by measuring the optic diameter and thickness of three post-cured implants using a caliper and calculating the difference with respect to the CAD model, reported as percentage.

### Physico-chemical characterization of the IOL-like implants

Thermal analysis was performed to evaluate the  $T_g$  and the thermal stability of the printed devices. The  $T_g$  was determined by DSC analysis in a DSC Q2500 instrument (TA

instruments, New Castle, USA). Samples with a mass of 1–3 mg were pressed into aluminum DSC pans that were introduced into the equipment used to perform the analysis. The samples were then subjected to a heating cycle from –50 to 150 °C, followed by a cooling step from 150 to –50 °C and a second heating ramp back to 150 °C. The scan rate for all cycles was 10 °C/min and the nitrogen flow was maintained constant at 50 mL/min. The data was analyzed using TRIOS software v4. 3. 1. 39215. The  $T_g$  value was obtained from the thermogram generated during the second heating cycle as the temperature at the midpoint of the decline in the heat capacity that takes place during this thermal event. The thermal stability of the lens-like 3D objects without refractive function was evaluated by TGA. This test was performed in a TGA 5500 system (TA Instruments, New Castle, DE, USA) under a nitrogen atmosphere. The sample was heated from 25 to 500 °C at a heating rate of 10 °C/min. The data were analyzed using TRIOS software v4. 3. 1. 39215 to determine the initial degradation temperature of the sample.

The absorption of water by the polymer was measured by performing a swelling test. Four implants were incubated in PBS 1× (0.5 mL, pH 7.4) at 35 °C for one month. The weights were recorded before the incubation and they were measured after 4, 24, and 48 h, one week, two weeks, and one month. Finally, the hydrophilicity/hydrophobicity of the material was evaluated by measuring the water contact angle using a goniometer built in-house. This device was composed of a red LED light source, a Hamilton needle, and a video camera (1080×768 pixels) connected to image capture software. The water contact angle was measured using ImageJ (NIH, Bethesda, MD, USA).

### Optical characterization

The spectral transmission curve of nine printed devices before and after 1 h of UV sterilization was measured using a FLUOstar® Omega microplate reader). A circular structure of 3 mm diameter was printed with the same resin composition as the IOL models and subsequently inserted into the wells of a 96-well tissue culture plate, after which they were immersed in 200 µL of borate buffer (0.1 M  $H_3BO_3$ , 75 mM NaCl and 25 mM  $Na_2[B_4O_5(OH)_4] \cdot 8H_2O$ , adjusted to pH 7). An absorbance scan was obtained from 300 to 800 nm wavelength at 2 nm resolution. A borate buffer was used as a blank. An absorbance scan was obtained and used to convert it to transmittance. Transmittance was calculated using the following formula:  $Transmittance = 10^{(2 \cdot Absorbance)}$ .

### Mechanical characterization

The haptic pull strength was measured using a Q800 dynamic mechanical analyzer (TA Instruments, Delaware, USA). A film-clamp was used and the oscillating frequency was set at 1 Hz. For the tensile tests, the haptic was fixed onto a plastic strip that was mounted in the clamp, allowing the force to distribute throughout the entire structure. Tensile experiments were carried out by pulling the haptic

with a ramp force of 0.25 N/min until fracture. A set of samples was measured at room temperature ( $n=4$ ), while another batch was analyzed at 37 °C after incubation in PBS at the same temperature for a week ( $n=4$ ).

### Morphological evaluation

Scanning electron microscopy (SEM) images of a post-cured implant were taken to evaluate the morphology of the central zone, haptics, and the edges. The samples were mounted on aluminum stubs and coated in an argon-filled sputter gold coater (Polaron SC7640, Quorum Technologies, UK) for 30 s before acquiring the images in a JEOL JSM 5900 LV microscope (Jeol Ltd., Tokyo, Japan) with a 20-kV accelerating voltage.

### Biocompatibility of the printed devices

The toxicity of the materials used in the manufacture of the lens-like 3D objects without refractive function was evaluated by performing a lactate dehydrogenase (LDH) cytotoxicity assay. The efficiency of the post-curing process in reducing the toxicity of the devices was also assessed by monitoring the changes in the biocompatibility of the polymers that occurred after each of the stages that comprised this treatment. A negative control group in which the cells were grown in the absence of an implant was also included in the experiment. Three tests, each with three technical replicates, were carried out to perform statistical analysis of the resulting data. FHL-124 cells were grown in 5% FCS-supplemented EMEM (PAN Biotech Ltd., Aidenbach, Germany) at 35 °C in a 5%  $CO_2$  incubator. This media had been further supplemented with L-glutamine and gentamicin. The 5% FCS-supplemented media was then removed and replaced with serum-free (SF) EMEM for 24 h. Following the period of serum starvation, the printed devices were pinned on top of the cells and the media was replaced with fresh SF EMEM. The dishes were then incubated at 35 °C in a 5%  $CO_2$  incubator. After 48 h, an LDH analysis was performed by following the protocol provided by the supplier (Roche, Basel, Switzerland). This study was repeated four times for each study group, and a total of three technical replicates were included in each experimental group.

### Implantation of the SLA-fabricated model in a human capsular bag ex vivo

A suspended human capsular bag system was used to evaluate the implantability. Donor human eye globes were obtained with UK National Research Ethics Committee approval (REC 04/Q0102/57) and used in accordance with the tenets of the Declaration of Helsinki. The procedure for the generation of the capsular bag model was first reported by Liu et al. in 1996<sup>26</sup> and is described in detail in the [Supplementary Information](#). After removing the lens fibers, a viscoelastic solution was injected into the capsular bag to

inflate it and facilitate the implantation of the IOL-like model. The SLA-fabricated implant was folded, loaded into a DualTec injector (Ophtec, Groningen, The Netherlands), and implanted into the capsular bag.

### Statistical analysis

The significance of the differences observed between the experimental groups analyzed in the cytotoxicity tests was evaluated by performing a one-way ANOVA analysis with a *post-hoc* Tukey test. The mean and standard deviation were calculated using Microsoft Excel<sup>®</sup> 2016 software. The statistical package GraphPad Prism v.6.01 was used for the statistical analysis. The level of significance was set at  $p < 0.05$ .

## Results

### Prototyping lens-like 3D objects without refractive function

Implantable devices which had been modeled on standard IOL designs were successfully produced by SLA. The CAD model of the lens-like 3D objects without refractive function was created using Blender. The model was based on a one-piece IOL with looped haptics; in this case, the optical part was flat on both faces (Figure 1). The haptic-to-haptic length was 13 mm, the optic diameter was 6 mm, and the thickness was set at 0.9 mm. A resin composed of 2-phenoxyethyl acrylate (POEA) and poly (ethylene glycol) dimethacrylate (PEGDMA) was employed in the manufacture of these devices. A pilot study was performed to optimize the composition of the resin. The formulation containing POEA 93% (w/w) and PEGDMA 7% (w/w) was

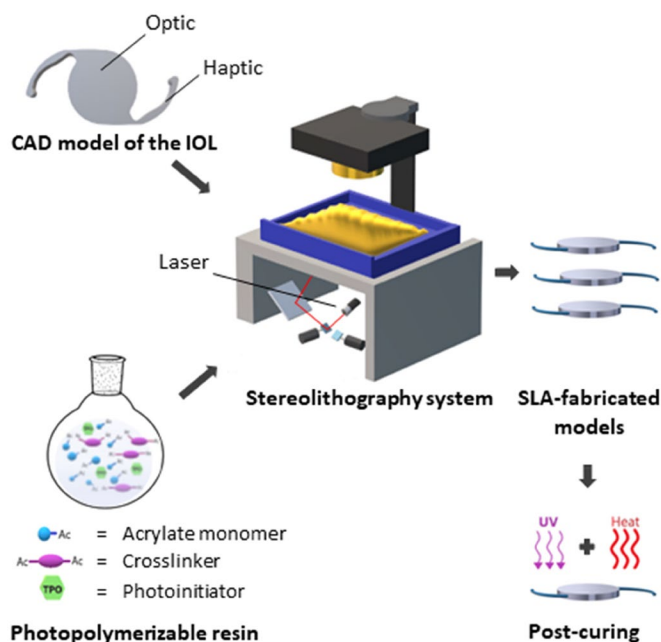


**Figure 1.** Schematic illustration of the production of lens-like 3D objects without refractive function by stereolithography. A resin composed of acrylate monomers and crosslinkers was developed and used for this purpose.

chosen for the fabrication of the implants. The photoinitiator was maintained at an additional 1% (w/w) in proportion to the total mass of the resin in all the formulations tested in these experiments (Figure S1, Supplementary Information).

Once fabricated, the dimensions of the implant were measured using a standard calibrated digital caliper. The compared accuracy of the dimensions between the printed devices and the CAD model was 94.5% for the optical diameter, with the thickness being 64% higher than the theoretical dimension of the CAD model. These data suggest that although the device was successfully fabricated, the accuracy of the dimensions was compromised.

### Assessment of the post-curing efficiency

The printed devices were subjected to a post-curing process to remove any unreacted monomers that remained within their polymeric structure. The efficiency of this process was monitored by incubating fully or partially post-cured samples in d-chloroform and subsequently detecting the monomers leached into the solvent using <sup>1</sup>H NMR. This experiment also served to determine the minimum time of UV irradiation and heating that was necessary to polymerize the residual monomers. The results showed that the amount of unreacted molecules decreased substantially after 1 h of UV irradiation, but it did not decrease any further with longer irradiation time (Figure 2). Thus, it was concluded that thermal post-curing was necessary to complete the polymerization of the monomers left within the polymer. As can be seen in the spectra, no monomer molecules were detectable after heating for 4 h in a vacuum.

### Physico-chemical characterization of the lens-like 3D objects without refractive function

The glass transition temperature ( $T_g$ ) of the printed polymers was assessed by DSC. According to the results (Figure 3(A)), the  $T_g$  of the crosslinked polymer that formed the printed devices was  $4.85 \pm 1.09^\circ\text{C}$ , which suggests that the materials may be rubbery and flexible at room temperature.

The thermal stability of the polymer was assessed by performing thermogravimetric analysis (TGA). According to the data (Figure 3(B)), the crosslinked polymer started to decompose at  $\sim 382.4 \pm 2.17^\circ\text{C}$ . The degradation occurred in one step which finished at  $\sim 450^\circ\text{C}$ . Finally, the behavior of the implants in an environment that was similar to that of the aqueous humor was assessed by performing a swelling test *in vitro*. The printed devices were incubated in PBS (pH 7.4) at  $35^\circ\text{C}$  for one month and their weights were recorded at different points. As their weight remained constant throughout the duration of the analysis (Figure 3(C)), it was concluded that the devices did not absorb any water due to their high hydrophobicity. This was corroborated by the high water contact angle measured *via* sessile drop technique, which had an average value of  $82.3 \pm 3.2^\circ$  (Figure S3, Supplementary Information). This is comparable to the water

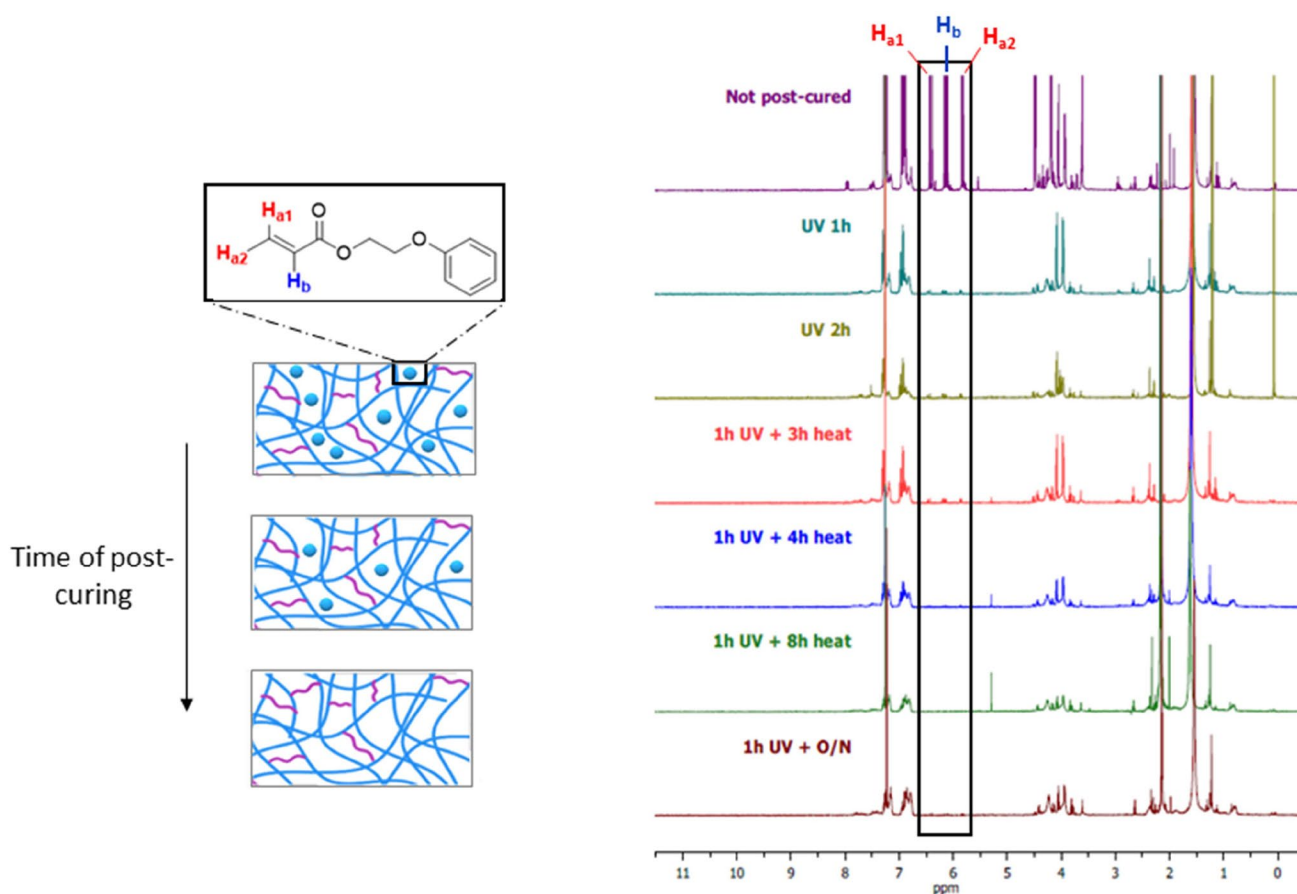


**Figure 2.**  $^1\text{H}$  NMR spectra obtained from the analysis of the incubation medium of printed IOL-like devices that had been subjected to different stages of the post-curing process (irradiation with 405-nm UV/visible light for 1 h and heat at  $80^\circ\text{C}$ ). The intensity of the signal at 4.8–5.2 ppm (highlighted in black rectangle), produced by the alkene groups from the remaining unreacted monomers that had leached out from the polymer, was reduced with longer time of post-curing.

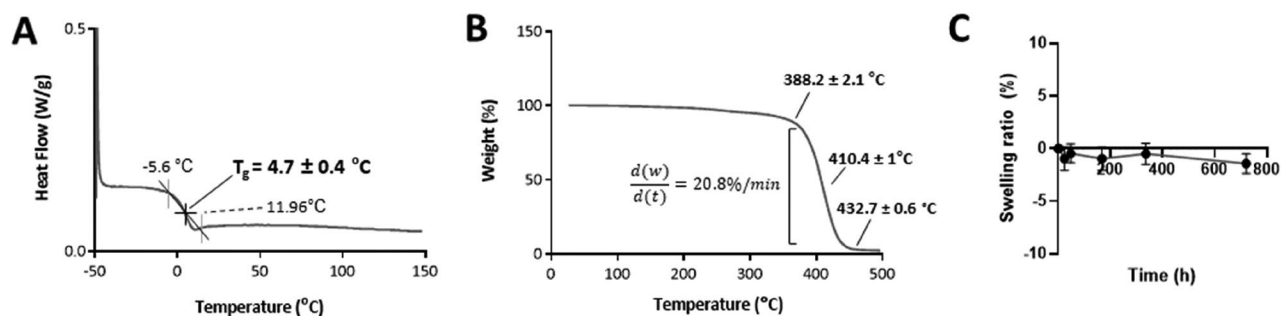


**Figure 3.** Physico-chemical characterization of the biomaterial that forms the SLA-fabricated implants. The  $T_g$  was obtained from the third heating cycle of the DSC analysis, the value being  $4.7 \pm 0.4^\circ\text{C}$  ( $n=3$ ) (A). The thermogram that resulted from the thermogravimetric analysis of the polymer shows that it started to degrade at  $388.2 \pm 2.1^\circ\text{C}$  ( $n=3$ ) (B). The line graph depicting the variation in the swelling ratio during a month shows that the polymer did not take up any water during this time period ( $n=4$ ) (C).

contact angle of the commercial IOL AcrySof, which is  $84.4 \pm 0.09^\circ$ .<sup>27</sup>

### Optical characterization

The transparency of the printed lens-like models was investigated by measuring the optical transmittance of the material. The results of this analysis showed that the implants transmitted 80–85% of the visible light that they

were exposed to (Figure 4(A)). The sterilization with UV light led to a 3% decrease in transmittance. The optical properties of the devices were also assessed by imaging them against a gridline background (Figure 4(B)). This showed that, in accordance with the results obtained from the transmittance measurements, the implants were relatively transparent and allowed the visualization of the gridlines.

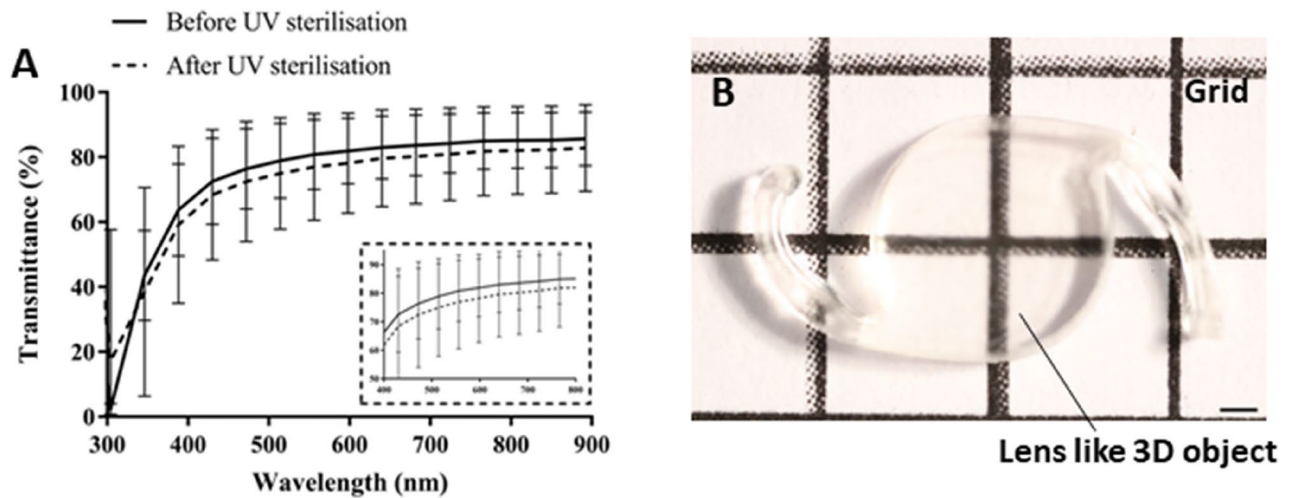


**Figure 4.** Optical characterization of the printed lens-like 3D objects. (A) Spectral transmittance of the devices before and after sterilization. A set of implants was sterilized for 1 h with UV irradiation and their light transmittance was compared to non-sterilized counterparts. The spectra indicate that the printed devices allow light transmission within the visible range (380–700 nm) and that the UV sterilization process slightly decreases the light transmittance by ~3%. Light transmittance (%) was obtained and represented against a wavelength range of 300–900 nm. Data are presented as mean  $\pm$  SD ( $n=9$ ). (B) Apparent visual clarity of a grid seen behind the IOL-like printed object. The scale bar represents 1 mm.

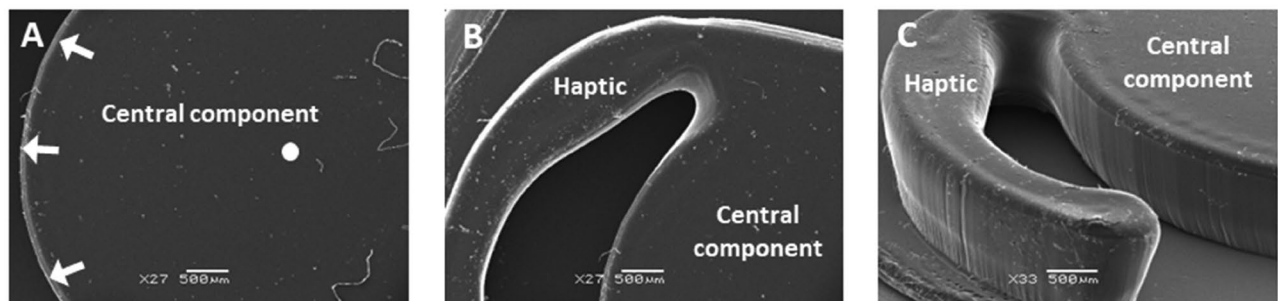


**Figure 5.** Scanning electron microscopy images showing the features of a printed and post-cured IOL-like implant. On the left, top-view of the central component, with white arrows highlighting the outer edge and a white circle marking the center of this part (A). In the middle, a top-view of the junction between the haptic and the central component (B). On the right, an image at an oblique angle of the central part and one of the haptics of the implant. Note that this image captures the vertical edge of the central component and the haptic (C).

### Mechanical characterization

The haptic tensile strength tests showed that the force that these structures withstand before becoming detached from the optic part is  $0.56 \pm 0.07$  N when dry (Figure S2(A) and Table S1, Supplementary Information) and that this decreases to  $0.39 \pm 0.05$  N after incubation in PBS at 37°C (Figure S2(B) and Table S2, Supplementary Information). In both conditions, they comply with the minimum of 0.25 N established by the ISO 11979-3.

### Morphological evaluation

The morphology of the printed lens-like objects was evaluated using scanning electron microscopy (SEM). The central component of the devices maintained a smooth circular shape and was relatively uniform on its upper surface (Figure 5(A)). Similarly, a clear definition of the haptic could also be observed (Figure 5(B)). The vertical edge of both the haptic and the optic-like part was flat and consistent. However, the point at which the vertical edge and the horizontal surfaces

met was rounded in appearance and did not form a sharp square-edge, which is a feature favored by several IOL manufacturers (Figure 5(C)).

### Biocompatibility of the printed implants

The effect of the post-curing process on the biocompatibility of the printed lens-like models was studied *in vitro*. Samples that had not been post-cured or which had been subjected to different stages of the post-curing protocol were co-incubated with FHL-124 lens cells for 48 h *in vitro*. After this time period, an LDH test was performed. The highest concentration of LDH in the media was detected in the cells that had been incubated with no post-cured polymer. These levels were significantly different from the control, as confirmed by the ANOVA and Tukey tests performed ( $p < 0.05$ ). Figure 6 shows that the LDH levels decreased significantly when the cells were cultured in the presence of polymers that had been post-cured with UV light. The level of cell death appeared to decrease further when the devices had

been heated in vacuum after being subjected to the UV irradiation step, such that cell death was not significantly different from cell only control cells. It was also observed that an increase in the duration of the heat treatment led to a reduction in the toxicity of the implants. The lowest cytotoxicity was detected when the polymeric devices had been heated overnight after UV irradiation. In this experimental group, the cell death levels were comparable to the cell-only

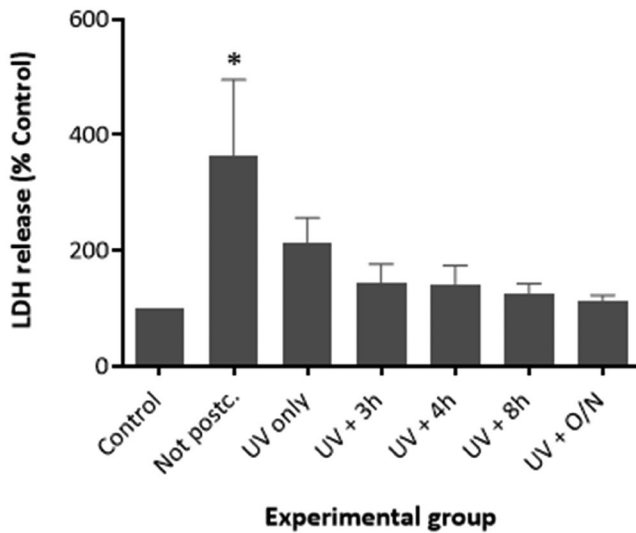


**Figure 6.** Cytotoxicity of the printed devices was analyzed by performing an LDH test with the lens cell line FHL-124. The results showed that the treatment of the lenses with UV/visible light (405 nm) and heating at 80°C reduces the cytotoxicity of the material. A significant increase in cell toxicity was only observed in the post-cured polymer group. The LDH release in all other treatment groups was comparable to the Control (No polymer). Cell toxicity was assessed by total LDH released using commercially available kit (Roche) after an incubation period of 48 h. The data are expressed as mean  $\pm$  SEM ( $n=9$ ) and were normalized to the control group. \* Indicates significant difference to control ( $p < 0.05$ , one-way ANOVA with Tukey's test).

negative control. Therefore, it was concluded that the devices must be irradiated with UV light for 1 h and heated in a vacuum overnight to minimize the toxicity elicited by these devices.

### Implantation of the SLA-fabricated lens-like models in a human capsular bag *ex vivo*

To provide clinical context, the printed lens-like objects were folded and loaded in an IOL injection system before ejection into a dish containing PBS (Figure 7). Following the ejection, the folded implant unfurled and recovered its natural shape without affecting the structural characteristics.

Having demonstrated that the printed devices can be successfully delivered with a clinical tool, the next step was to show that a printed prototype could be implanted within the capsular bag (Figure 8). To demonstrate this, a human capsular bag model was used. This system is generated by performing a sham cataract surgery *ex vivo*. A printed lens-like object was successfully implanted into the capsular bag using a standard IOL injector without rupturing the capsule. The implant was well-centered and did not cause undue deformation of the capsular bag.

### Discussion

While current IOL manufacturing technology generates high-quality products, there is considerable scope to advance the prototyping and fabrication methods. In current practice, the production of a novel design requires the fabrication of new molds or other specialist equipment, with the associated expenses and lengthy manufacturing times. Furthermore, the large space required to accommodate the manufacturing equipment makes it less accessible for researchers. This hinders the development of novel IOLs with designs and

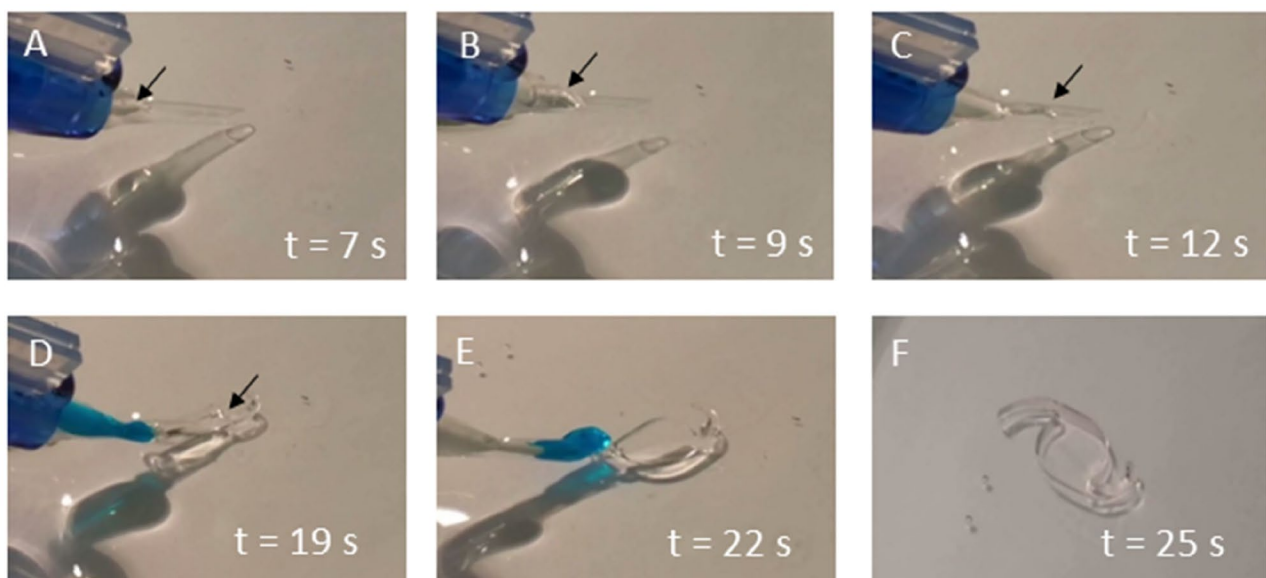


**Figure 7.** Multiple frames of a digital video showing the delivery of a lens-like 3D object from a surgical injector. The first three images (A–C) show the prototype, indicated with an arrow, inside the injector and being delivered to the aqueous medium. The implant unfolds upon release from the injector (D,E) until it recovers its original shape (F).



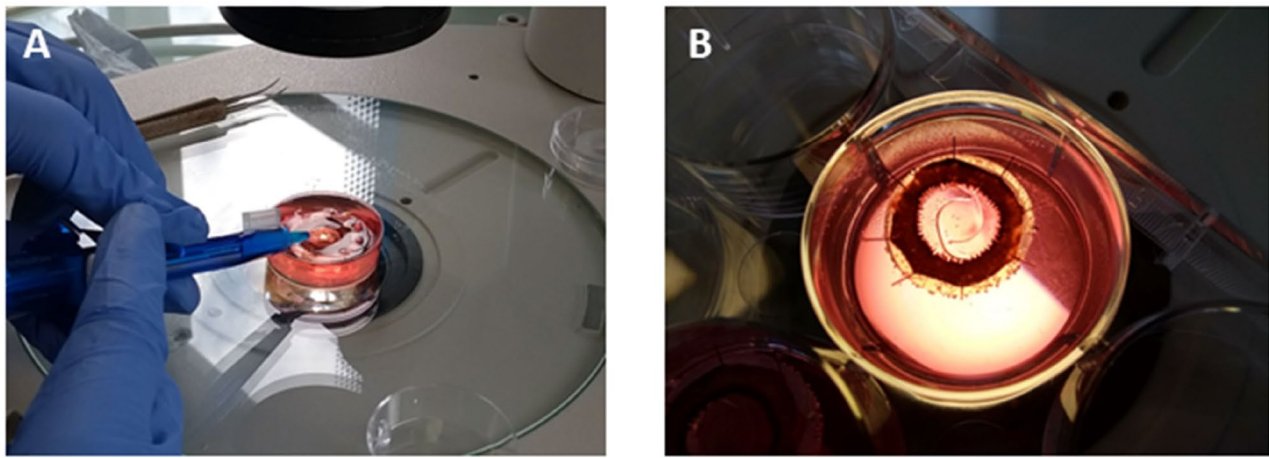


**Figure 8.** Digital images showing the implantation of a printed IOL-like device in a human capsular bag model *in vitro*. The delivery of the implant into the capsular bag can be seen in image (A). Once implanted in the capsular bag, the implant recovered its original shape without causing any deformation in this structure (B).

formulations that can prevent post-operative complications. The rapid fabrication of IOLs using SLA could accelerate the prototyping process, eliminating the need for molding or extensive lathing procedures. While previous studies have attempted to use SLA to produce IOLs, these did not provide a quantitative assessment of the dimensional accuracy, mechanical properties, and cytocompatibility. Thus, the functionality of the resulting implants was not demonstrated. The proof-of-principle study reported herein aimed at demonstrating the production of IOL prototypes by using SLA technology and the potential of the printable materials to form IOLs that can fulfill certain requirements, such as biocompatibility and mechanical strength. We also analyzed the aspects that need to be improved before considering the progression to further stages in their application. To demonstrate the process, we fabricated a standard IOL design with an optical zone and looped haptics. We chose POEA as the main monomer and PEGDMA as a crosslinker to fabricate the IOL-like implant. POEA is suitable as this is an aromatic-based monomer with a relatively high refractive index (1.52), whereas PEGDMA is an aliphatic bifunctional crosslinker incorporated into the mixture to obtain prototypes with suitable mechanical properties.

Once the IOL-like models were printed, the accuracy between the theoretical and physical dimensions was investigated. Although all the parts of the implant were successfully fabricated, the physical dimensions of the printed devices were different from those of the CAD model. The average accuracy of the central component diameter of the SLA-fabricated models was  $94.5 \pm 0.4\%$ . However, the thickness of the device was  $64 \pm 7.8\%$  higher than that of the CAD model. This suggests that further optimization is required to limit the penetration depth of the UV light into the resin. The use of a build platform would have been beneficial to limit the cure depth, but it would lead to a layer-by-layer fabrication that would compromise the optical quality of the objects. However, the continuing innovation in the 3D-printing industry has led to the development of high-resolution printers that incorporate features that make

them more compatible with the manufacture of optical devices. The use of such systems for the manufacture of IOLs, together with the formulation and characterization methods reported in this work, could accelerate the process of creating new IOL prototypes and taking them forward to pre-clinical testing stages.

Next, we subjected the printed lens-like objects to a post-curing process to complete the polymerization of any unreacted monomers or polymer chains, as this would improve the mechanical strength and biocompatibility. The devices were post-cured by irradiating them with UV light and heating them in a vacuum oven at  $70^\circ\text{C}$ . The exposure to UV light activates the formation of chemical bonds between the unreacted monomers and the polymer chains. Heating under vacuum accelerates this process while preventing the inhibitory effects exerted by oxygen. An NMR analysis and an LDH cytotoxicity test revealed that the optimal post-curing time required to ensure the depletion of unreacted monomers was 1 h of UV irradiation, followed by an overnight incubation in the vacuum oven. The cytotoxicity assay indicated that the toxicity levels elicited by polymeric implants that had not been post-cured were significantly higher than those of the negative control, which did not contain any device in contact with the cells. On the other hand, the implants that had been post-cured overnight caused substantially lower levels of cell death, which were comparable to those of the negative control. Therefore, we concluded that the post-curing protocol increased the biocompatibility of the printed devices by eliminating the unreacted monomers that remained within the polymer after SLA.

The suitability of the fabricated prototypes for use in cataract surgery was assessed by performing a physicochemical characterization. The equilibrium water content was calculated by performing a swelling test in an aqueous medium at  $35^\circ\text{C}$ , which is the temperature of the human eye. Due to their hydrophobic nature, the lens-like models did not take up any water in their polymeric structure. This could be beneficial for preventing the glistenings reported in some

IOLs and for the lenses to maintain their dimensions once implanted in the capsular bag. The transparency of the devices was evaluated *via* optical imaging and by measuring the spectral transmittance. This showed that they were optically clear, although their transparency was ~10% lower than that of the AcrySof IOL.<sup>28</sup> However, it is important to note that we did not incorporate a polishing step into the manufacturing process.

Other characteristics required for an IOL to be employed in cataract surgery include the ability to fold/unfold and the resistance of the haptics to a force of 0.25 N before detaching from the optic. This would allow the implant to withstand the mechanical stress that it is subjected to during the injection through a small incision. The DSC analysis of the printed samples reveals that the polymer used in the manufacturing of intraocular lenses (IOLs) exhibits a glass transition temperature ( $T_g$ ) at  $4.7 \pm 0.4^\circ\text{C}$ . The determination of the  $T_g$  is crucial, as it denotes the temperature at which the polymer shifts from a hard and brittle disposition to a more pliable and flexible state. This flexibility is imperative for IOLs, given the necessity for them to be foldable for insertion through the small incision made during cataract surgery. The consistency of the  $T_g$ , suggested by its narrow range, ensures that the polymer will behave predictably during the critical folding and insertion phases.

Moreover, the DSC curve provides an onset temperature of  $-5.6^\circ\text{C}$  and an endset at  $11.96^\circ\text{C}$ , indicating that the polymer starts softening at temperatures well below room level and maintains flexibility above the normal physiological temperature. This characteristic is vital for the manipulation of IOLs during surgery, as it allows for easy handling without compromising the material's ability to return to its original shape once positioned inside the eye.

Corroborating the DSC data, our mechanical testing has shown that the haptics of the IOL are capable of withstanding a tensile force significantly  $>0.25\text{ N}$  threshold before detachment from the optic part occurs. This robustness in both thermal and mechanical aspects is essential to withstand the mechanical stress imposed during injection through a small incision, particularly in the phacoemulsification technique for IOL implantation. Further chemical characterization included TGA, which confirmed that the polymer that formed the implants had a high thermal stability. The morphology of the printed devices was evaluated by SEM. The images obtained with this technique showed the successful fabrication of all the parts of the device with a relatively good resolution. Generally, the surfaces of the devices are smooth and flat, although the square-edge that is desirable for the prevention of secondary cataract was not formed in these models.

Finally, we performed an implantation test using an *ex vivo* human capsular bag model to evaluate the resistance of these devices to the mechanical stress exerted on them during injection. The SLA-fabricated lens-like object was injected into the capsular bag using a surgical injector. The implantability of these devices in human eyes using clinical instrumentation was thus demonstrated, as they had the appropriate flexibility and mechanical strength

required for them to withstand the forces that they were subjected to during this process. Furthermore, it was also confirmed that the size of the implants was adequate for implantation without abnormal stretching or deformation of the capsular bag, which could potentially affect the optical performance.

## Conclusions

This proof-of-principle study demonstrates that SLA can be used to directly and rapidly fabricate IOL-like objects with relatively high accuracy, good transparency, foldability, and biocompatibility. We have shown that IOLs could be rapidly prototyped without the requirement to first develop specific IOL molds or extensive lathing processes. Thus, this would facilitate the creation of novel IOL designs that would be very difficult to prototype with traditional manufacturing methods. The models that resulted from this study were optically clear, hydrophobic and they fulfilled the requirements for haptic pull strength established by the ISO 11979-3. The LDH analysis performed *in vitro* confirmed the absence of toxic responses in the cells that were cultured in contact with post-cured polymeric devices. We have also shown the foldability and implantability of the fabricated devices in an advanced human capsular bag model *in vitro*. However, further work is needed to increase the printing resolution to improve the dimensional accuracy. Other aspects that need to be optimized in the future include the scalability and reproducibility of the process.

## Author contributions

**Aram Saeed** co-conceived the original idea and led the invention from its ideation through to design, engineering of materials, method development, and application in ocular devices. He was instrumental in all patentable aspects, from formulation design to experimental execution, data analysis, and manuscript writing. Aram Saeed supervised the project as the Principal Investigator, directing the contributions of other team members towards the realisation of the invention.

**Michael Wormstone** co-conceived the original idea with Aram Saeed and was crucial in applying the invention in human-eye capsular bags, ensuring the practical applicability of the patent claims. He also contributed to the revision of the manuscript, co-supervised the project, and engaged in critical scientific discussions that shaped the final output.

**Veronica Hidalgo-Alvarez** working under the direction of Aram Saeed, executed specific tasks in additive manufacturing and characterization and assisted in data analysis and manuscript editing, as per the project requirements set by the lead inventors.

**Noelia D. Falcon** performed specific additive manufacturing processes and optical testing as instructed, contributing to the practical testing phases of the project under the supervision of Aram Saeed.

**Julie Eldred** was assigned to perform the toxicological analysis critical to the project's safety assessments. Her contributions to the manuscript were focused on the revision of the sections pertaining to toxicology under the guidance of the principal investigators.

## Disclosure statement

(P) Aram Saeed and Michael Wormstone are credited as inventors in a patent family associated with this research, which has been assigned to UEA Enterprise Limited. The extent of their contributions to this work

varied. The patent family includes the granted US patent 11958927, along with its international counterparts WO2020049307A1 and EP3846865A1.

## Funding

Financial support for this research was provided to Aram Saeed and Michael Wormstone by the following sources: the University of East Anglia through the Innovation Development Fund and Proof-Of-Concept grants (Grant numbers: R202499); the Humane Research Trust; and the Engineering and Physical Sciences Research Council (EPSRC) through Grant EP/S021485/1. We gratefully acknowledge the further funding provided by the UEA MRC Impact Acceleration Account (IAA), which has been instrumental in advancing this work.

## ORCID

Aram Saeed  <http://orcid.org/0000-0003-2903-5875>

## Data availability statement

The data that support the findings of this study are available from the corresponding author, [AS], upon reasonable request.

## References

- Prokofyeva E, Wegener A, Zrenner E. Cataract prevalence and prevention in Europe: a literature review. *Acta Ophthalmol.* 2013;91(5):395–405. doi: [10.1111/j.1755-3768.2012.02444.x](https://doi.org/10.1111/j.1755-3768.2012.02444.x).
- Wormstone IM, Wormstone YM, Smith AJO, Eldred JA. Posterior capsule opacification: what's in the bag? *Prog Retin Eye Res.* 2021;82:100905. doi: [10.1016/j.preteyeres.2020.100905](https://doi.org/10.1016/j.preteyeres.2020.100905).
- Toh T, Morton J, Coxon J, Elder MJ. Medical treatment of cataract. *Clin Exp Ophthalmol.* 2007;35(7):664–671. doi: [10.1111/j.1442-9071.2007.01559.x](https://doi.org/10.1111/j.1442-9071.2007.01559.x).
- Jin C, Chen X, Law A, Kang Y, Wang X, Xu W, Yao K. Different-sized incisions for phacoemulsification in age-related cataract. *Cochrane Database Syst Rev.* 2017;9:CD010510.
- Leyland M, Zinicola E. Multifocal versus monofocal intraocular lenses in cataract surgery: a systematic review. *Ophthalmology.* 2003;110(9):1789–1798. doi: [10.1016/S0161-6420\(03\)00722-X](https://doi.org/10.1016/S0161-6420(03)00722-X).
- Wormstone IM, Eldred JA. Experimental models for posterior capsule opacification research. *Exp Eye Res.* 2016;142:2–12. doi: [10.1016/j.exer.2015.04.021](https://doi.org/10.1016/j.exer.2015.04.021).
- Singh B, Sharma S, Bharti N, Samantrey D, Paandey DJ, Bharti S. Visual and refractive outcomes of new intraocular lens implantation after cataract surgery. *Sci Rep.* 2022;12(1):14100. doi: [10.1038/s41598-022-14315-6](https://doi.org/10.1038/s41598-022-14315-6).
- Pedrotti E, Carones F, Aiello F, Mastropasqua R, Bruni E, Bonacci E, Talli P, Nucci C, Mariotti C, Marchini G. Comparative analysis of visual outcomes with 4 intraocular lenses: monofocal, multifocal, and extended range of vision. *J Cataract Refract Surg.* 2018;44:156–167.
- Bozukova D, Pagnouille C, Jérôme R, Jérôme C. Polymers in modern ophthalmic implants—historical background and recent advances. *Mater Sci Eng R Rep.* 2010;69(6):63–83. doi: [10.1016/j.mser.2010.05.002](https://doi.org/10.1016/j.mser.2010.05.002).
- Luo C, Wang H, Chen X, Xu J, Yin H, Yao K. Recent advances of intraocular lens materials and surface modification in cataract surgery. *Front Bioeng Biotechnol.* 2022;10:913383. doi: [10.3389/fbioe.2022.913383](https://doi.org/10.3389/fbioe.2022.913383).
- Olson RJ, Werner L, Mamalis N, Cionni R. New intraocular lens technology. *Am J Ophthalmol.* 2005;140(4):709–716. doi: [10.1016/j.ajo.2005.03.061](https://doi.org/10.1016/j.ajo.2005.03.061).
- Kumari R, Srivastava M, Garg P, Janardhanan R. Intra ocular lens technology—a review of journey from its inception. *Ophthalmol Res.* 2020;11:1–9. doi: [10.9734/or/2019/v11i330129](https://doi.org/10.9734/or/2019/v11i330129).
- Yu N, Fang F, Wu B, Zeng L, Cheng Y. State of the art of intraocular lens manufacturing. *Int J Adv Manuf Technol.* 2018;98(5–8):1103–1130. doi: [10.1007/s00170-018-2274-5](https://doi.org/10.1007/s00170-018-2274-5).
- Yildirim TM, Fang H, Schickhardt SK, Wang Q, Merz PR, Auffarth GU. Glistening formation in a new hydrophobic acrylic intraocular lens. *BMC Ophthalmol.* 2020;20(1):186. doi: [10.1186/s12886-020-01430-z](https://doi.org/10.1186/s12886-020-01430-z).
- Weinschenk JIII, Deacon J, Sussman GR. Method of producing repositionable intraocular lenses. United States Patent 5,567,365. Allergan, Inc.; 1996. <https://patents.justia.com/inventor/joseph-i-weinschenk?page=3>.
- Tripti D, Haldar RS, Geetha S, Niyogi UK, Khandal RK. Materials for intraocular lenses (IOLs): review of developments to achieve biocompatibility. *e-Polymers.* 2009;9(1). doi: [10.1515/epoly.2009.9.1.1466](https://doi.org/10.1515/epoly.2009.9.1.1466).
- Glick RE, Deacon J, Kent BW. Cast molding of intraocular lenses. United States Patent 5,620,720. Allergan, Inc.; 1997.
- Sarbadhikari KK. Intraocular lens manufacturing apparatus. United States Patent 6,732,994 B2. Bausch & Lomb Incorporated; 2004.
- Selimis A, Mironov V, Farsari M. Direct laser writing: principles and materials for scaffold 3D printing. *Microelectron Eng.* 2015;132:83–89. doi: [10.1016/j.mee.2014.10.001](https://doi.org/10.1016/j.mee.2014.10.001).
- Wang X, Jiang M, Zhou Z, Gou J, Hui D. 3D printing of polymer matrix composites: a review and prospective. *Compos Part B Eng.* 2017;110:442–458. doi: [10.1016/j.compositesb.2016.11.034](https://doi.org/10.1016/j.compositesb.2016.11.034).
- Sun Q, Fang F, Wang W, Yin J, Liu Q, Hao L, Peng Y. Stereolithography 3D printing of transparent resin lens for high-power phosphor-coated WLEDs packaging. *J Manuf Process.* 2023;85:756–763. doi: [10.1016/j.jmapro.2022.11.026](https://doi.org/10.1016/j.jmapro.2022.11.026).
- Chartrain NA, Williams CB, Whittington AR. A review on fabricating tissue scaffolds using vat photopolymerization. *Acta Biomater.* 2018;74:90–111. doi: [10.1016/j.actbio.2018.05.010](https://doi.org/10.1016/j.actbio.2018.05.010).
- Debellemanniè G, Flores M, Montard M, Delbosc B, Saleh M. Three-dimensional printing of optical lenses and ophthalmic surgery: challenges and perspectives. *J Refract Surg.* 2016;32(3):201–204. doi: [10.3928/1081597X-20160121-05](https://doi.org/10.3928/1081597X-20160121-05).
- Li JW, Li YJ, Hu XS, Gong Y, Xu BB, Xu HW, Yin ZQ. Biosafety of a 3D-printed intraocular lens made of a poly(acrylamide-co-sodium acrylate) hydrogel *in vitro* and *in vivo*. *Int J Ophthalmol.* 2020;13(10):1521–1530. doi: [10.18240/ijjo.2020.10.03](https://doi.org/10.18240/ijjo.2020.10.03).
- Kumagai H, Arai M, Gong J, Sakai K, Kawakami M, Furukawa H. Modeling the transparent shape memory gels by 3D printer Acculas. SPIE; 2016. <https://www.spiedigitallibrary.org/conference-proceedings-of-spie/9802/1/Modeling-the-transparent-shape-memory-gels-by-3D-printer-Acculas/10.1117/12.2218236.short>.
- Liu CS, Wormstone IM, Duncan G, Marcantonio JM, Webb SF, Davies PD. A study of human lens cell growth *in vitro*. A model for posterior capsule opacification. *Invest Ophthalmol Visual Sci.* 1996;37:906–914.
- Jung GB, Jin K-H, Park H-K. Physicochemical and surface properties of acrylic intraocular lenses and their clinical significance. *J Pharm Investig.* 2017;47(5):453–460. doi: [10.1007/s40005-017-0323-y](https://doi.org/10.1007/s40005-017-0323-y).
- Li X, Kelly D, Nolan JM, Dennison JL, Beatty S. The evidence informing the surgeon's selection of intraocular lens on the basis of light transmittance properties. *Eye.* 2017;31(2):258–272. doi: [10.1038/eye.2016.266](https://doi.org/10.1038/eye.2016.266).